JACS
JOURNAL OF THE AMERICAN CHEMICAL SOCIETY

COMMUNICATION

pubs.acs.org/JACS

Segregated Donor−Acceptor Columns in Liquid Crystals That Exhibit Highly Efficient Ambipolar Charge Transport

Hironobu Hayashi,[†] Wataru Nihashi,[†] Tomokazu Umeyama,[†,⊥] Yoshihiro Matano,[†] Shu Seki,[*,#,⊥] Yo Shimizu,[*,∥] and Hiroshi Imahori[*,†,‡,§]

[†]Department of Molecular Engineering, Graduate School of Engineering and [‡]Institute for Integrated Cell-Material Sciences (iCeMS), Kyoto University, Nishikyo-ku, Kyoto 615-8510, Japan

[⊥]PRESTO, Japan Science and Technology Agency, 4-1-8 Honcho, Kawaguchi, Saitama 332-0012, Japan

[#]Department of Applied Chemistry, Graduate School of Engineering, Osaka University, 2-1, Yamadaoka, Suita, Osaka 565-0871, Japan

[∥]National Institute of Advanced Industrial Science and Technology, Kansai-Center, 1-8-31 Midorigaoka, Ikeda, Osaka 563-8577, Japan

[§]Fukui Institute for Fundamental Chemistry, Kyoto University, Sakyo-ku, Kyoto 606-8103, Japan

Supporting Information

ABSTRACT: Liquid crystalline donor (i.e., phthalocyanine) was covalently linked to acceptor (i.e, fullerene) to achieve efficient charge-transport properties in a liquid crystalline phase. The columnar structure exhibited highly efficient ambipolar charge-transport character, demonstrating the potential utility of the strategy in organic electronics.

Recently liquid crystals (LCs) have drawn much attention as a promising type of molecular semiconductor because of their potential utility in organic electronics including organic thin-film transistors, organic light-emitting diodes, and organic solar cells.[1] Disc-like molecules functionalized with alkyl groups self-assemble into supramolecular one-dimensional (1D) columns that further self-organize into hexagonal, rectangular, and nematic phases as discotic liquid crystals (DLCs).[2] Hierarchical self-assembly from simple disc-like molecules to DLCs through the formation of 1D columns is a highly appealing strategy to organize donor−acceptor (D−A) molecules,[3] i.e., forming D−A heterojunction structures exhibiting ambipolar charge-transport properties[4] and efficient photocurrent generation.[5]

As donors, phthalocyanines are some of the most widely investigated self-assembling molecules in DLCs.[2,6] As acceptors, fullerenes have been successfully incorporated into LC systems to give various LC phases.[7] Some of the covalently functionalized fullerenes are known to form different columnar phases.[8] Therefore, a simultaneous application of a phthalocyanine and a fullerene to LCs is highly attractive to form such D−A heterojunction structures. So far there have been only a few examples of mesogenic phthalocyanine−fullerene linked dyads.[9] As such, relationships between the LC structures and charge-transport properties have yet to be examined.

Herein we report the synthesis and LC and charge-transport properties of a zinc phthalocyanine (ZnPc)−C_{60} dyad (Figure 1). Six 4-dodecyloxyphenoxy groups were introduced into the periphery of the central core to form the discotic columnar structure of the ZnPc.[10] C_{60} was also tethered to the ZnPc core via a short, semiflexible bridge. We expected that, due to the strong $\pi-\pi$ interaction between the C_{60} molecules and the covalent linkage, the C_{60} molecules would be arranged successively along the ZnPc 1D column, leading to D−A bicontinuous structure in the LCs.

The synthesis and characterization of ZnPc−C_{60} and zinc phthalocyanine reference (ZnPc-ref) are described in the Supporting Information (SI). The LC properties of ZnPc−C_{60} and ZnPc-ref were examined by a combination of differential scanning calorimetry (DSC), polarized optical microscopy (POM), and X-ray diffraction (XRD). Upon heating, only one broad endothermic curve (35−80 °C) with a peak of ca. 53 °C, corresponding to the LC-like phase-to-LC phase transition, is seen in ZnPc−C_{60}, whereas that corresponding to the crystal-to-LC phase transition is observed at 124 °C in ZnPc-ref (SI, Figure S1 and Table S1). Once ZnPc−C_{60} and ZnPc-ref were heated above the respective transition temperature, they formed a glassy LC state at 25 °C. Two POM images of ZnPc-ref at 25 and 160 °C show similar optical textures, while those of ZnPc−C_{60} reveal a birefringence texture upon heating to 160 °C (Figure S2). After being cooled to 25 °C, both ZnPc-ref and ZnPc−C_{60} showed birefringence textures similar to those at 160 °C. These results corroborate that ZnPc-ref and ZnPc−C_{60} retain the mesophases consisting of the ordered structures (i.e., glassy LC state) at 25 °C. These mesophases were identified by XRD (Figure 2 and Table S2). Upon heating ZnPc-ref to 160 °C, its XRD patterns exhibit hexagonal columnar (Col_h) mesophase (Figure 2a,b). On the other hand, XRD patterns of ZnPc−C_{60} at 25 °C (Figure S3a,b) and 160 °C (Figure 2c,d) are rather similar, but when the sample is heated to 160 °C, the peak intensities are remarkably enhanced, leading to the change from LC-like phase (Col_r1) to discotic rectangular columnar mesophase (Col_r2). Additionally, ZnPc−C_{60} retains this ordered structure after cooling to 25 °C (Figure S3c,d). Considering a broad reflection peak of (001) in ZnPc−C_{60}, the ZnPc part in ZnPc−C_{60} may form a disordered column in the Col_r2 mesophase, although such disordered columns of phthalocyanines are reported to reveal high hole mobility ($\sim 10^{-1}$ cm^2 V^{-1} s^{-1}).[11] We also measured the absorption spectra of the ZnPc-ref and ZnPc−C_{60} films to get information on the packing geometries of the ZnPc moieties in the film after heating and cooling treatment (Figure S4). Both spectra show a blue-shift of

Received: April 26, 2011
Published: June 23, 2011

dx.doi.org/10.1021/ja203822q | J. Am. Chem. Soc. 2011, 133, 10736–10739

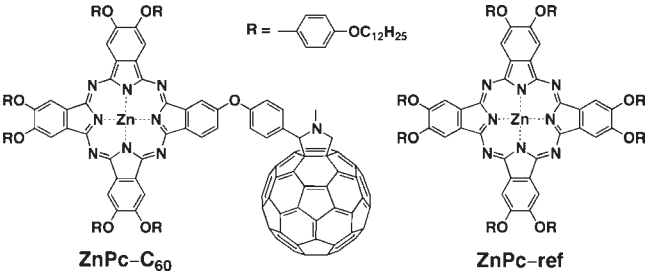

Figure 1. Phthalocyanine derivatives used in this study.

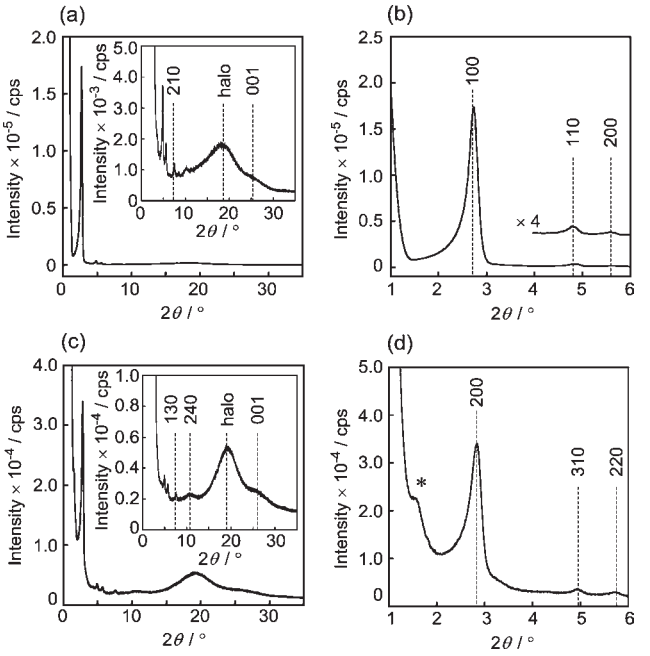

Figure 2. XRD patterns of ZnPc-ref in 2θ ranges of (a) 0−35° and (b) 1−6°, and of ZnPc−C_{60} in 2θ ranges of (c) 0−35° and (d) 1−6°. Each sample was measured at 160 °C. The intensified XRD patterns in 2θ ranges of 0−35° are also depicted as insets in (a) and (c). The asterisk in Figure 2d marks a peak arising from a helical pitch of C_{60} molecules along the ZnPc column.

the absorption arising from the ZnPc moiety relative to those in toluene, supporting the face-to-face stacking of the ZnPc moieties in the discotic columnar structures.

It is noteworthy that only ZnPc−C_{60} reveals a low-angle peak at 1.59° (asterisk in Figure 2d) that can be assigned as a helical pitch of molecules (5.48 nm), 16 times the layer spacing of 0.34 nm.[12] These results suggest that, due to the $\pi-\pi$ interaction, C_{60} molecules are also arranged linearly, showing helical alignment along the ZnPc columnar structures. To shed light on the C_{60} arrangement, XRD measurements were also performed for the uniaxially oriented films of ZnPc−C_{60} (Figure S5).[13] These oriented films were prepared by uniaxial shearing of the sample surface. When the direction of the X-ray is parallel to the axis of the ZnPc column, the peak assigned to the helical pitch becomes more evident, supporting the helical C_{60} arrangement along the ZnPc column. Interestingly, the integrated areas of the peak assigned to helical pitch extracted by peak fitting are rather comparable before and after heat treatment (Figure S3e,f). This implies that this helical C_{60} arrangement along the ZnPc column

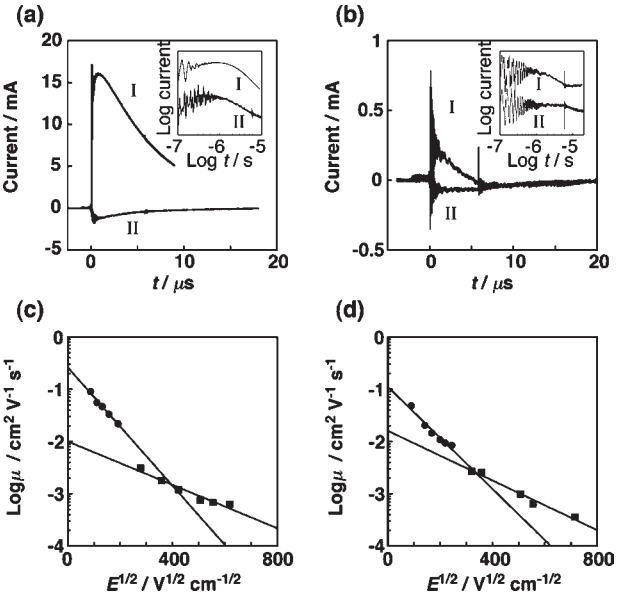

Figure 3. TOF current transients observed for ZnPc−C_{60} (a) before heating at an electric field strength (E) of 1.3×10^5 V cm^{-1} and (b) at 25 °C, after the sample was heated to 160 °C for 10 min and then cooled to 25 °C at $E = 7.7 \times 10^3$ V cm^{-1} after photoexcitation with a 355 nm laser pulse. Curves I and II were observed under positive and negative bias, respectively. The log−log plots of TOF current transients vs time are also depicted as insets in (a) and (b). (c) Log hole and (d) log electron mobilities observed for ZnPc−C_{60} as a function of $E^{1/2}$, (■) before and (●) after the sample was heated, respectively.

Table 1. Charge Mobilities of ZnPc-ref and ZnPc−C_{60}[a]

compound	TOF μ_h, cm^2 V^{-1} s^{-1}	TOF μ_e, cm^2 V^{-1} s^{-1}	TRMC $\sum\mu$, cm^2 V^{-1} s^{-1}
ZnPc-ref	2.8 (−)[b]	0 (−)[b]	3.0 (7.3)
ZnPc−C_{60}	0.26 (0.010)	0.11 (0.016)	0.52 (0.10)

[a] The values in parentheses were obtained before the heating procedure. [b] Could not be measured.

is formed even before heating, due to the plausible self-assembling process in the reprecipitation procedure by toluene and methanol as reported previously (vide infra).[4f,5a,5c]

To correlate the LC structures with the charge-transport properties, electron mobility (μ_e) and hole mobility (μ_h) were determined by the time-of-flight (TOF) method (Figures 3 and S6 and SI). Electron and hole mobilities under the electric field (E = 0) were obtained by extrapolation from the plots of the corresponding mobilities as a function of $E^{1/2}$ (Figure 3c,d). The μ_e and μ_h values of ZnPc-ref could not be obtained before the sample was heated because of the poor film formation. After heating and cooling treatment, ZnPc-ref had a high μ_h value of 2.8 cm^2 V^{-1} s^{-1} but did not show electron mobility (Figure S6 and Table 1). In contrast, the current transients of ZnPc−C_{60} film before and after heating were observed under both positive and negative bias (Figure 3a,b), suggesting ZnPc−C_{60} exhibits ambipolar charge-transport character with rather comparable μ_h and μ_e values. The electron mobility of the ZnPc−C_{60} film before heating is larger than the hole mobility, showing that an electron-transporting pathway (i.e., the helical C_{60} arrangement along the ZnPc column) is formed before heating (vide supra). It should be noted here that the respective μ_h and μ_e values increase

dx.doi.org/10.1021/ja203822q | J. Am. Chem. Soc. 2011, 133, 10736–10739

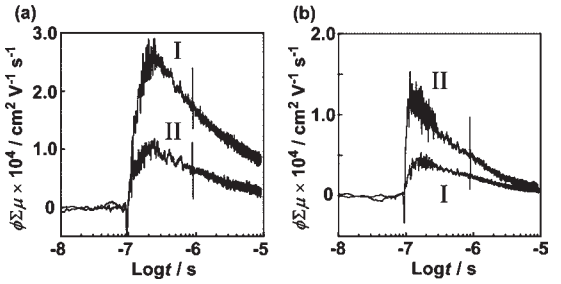

Figure 4. (a) TRMC profiles of ZnPc-ref before heating (curve I) and at 25 °C, after the sample was heated to 160 °C for 10 min and then cooled to 25 °C (curve II). (b) TRMC profiles of ZnPc−C_{60} before heating (curve I) and at 25 °C, after the sample was heated to 160 °C for 10 min and then cooled to 25 °C (curve II), after photoexcitation with 355 nm laser pulse.

by 26 and 7 times after the heating and cooling treatment. This shows that heating allows the ZnPc−C_{60} molecules to adopt more regular arrangement, especially the intracolumn arrangement of the ZnPc moiety as well as the intercolumn arrangement, leading to improvement of the ambipolar charge-transport properties. More importantly, ZnPc−C_{60} displays remarkably high $\mu_h = 0.26$ cm^2 V^{-1} s^{-1} and $\mu_e = 0.11$ cm^2 V^{-1} s^{-1}, which are the highest values ever reported for organic materials with D−A heterojunction.[4,5a] Meanwhile, the log charge mobilities decrease with increasing electric fields (Figure 3c,d). The negative E-field dependency of charge mobility indicates that carrier trapping occurs with a larger probability as the applied voltage is larger and generally arises when different hopping processes with different activation energies operate. Given that the macroscopic charge-carrier transport in the sample should involve both intracolumn (much less energy-demanding) and intercolumn (much more energy-demanding) hopping events, the observed negative E-field dependency of the charge mobility seems reasonable.[4f,14]

With these contrasting long-range charge-transport properties in mind, we measured flash-photolysis time-resolved microwave conductivities (TRMC) of ZnPc-ref and ZnPc−C_{60} (Figure 4 and SI). This electrodeless method allows for evaluating short-range transient conductivities of materials.[15] For instance, upon exposure to a 355 nm laser pulse at 25 °C, ZnPc-ref reveals a prompt increase of a transient conductivity, $\langle \phi\Sigma\mu \rangle$, in which ϕ is the quantum efficiency of charge separation and $\Sigma\mu$ is the sum of mobilities of all the transient charge carriers, thus reaching maximum transient conductivities of 2.9×10^{-4} cm^2 V^{-1} s^{-1} before heating and 1.2×10^{-4} cm^2 V^{-1} s^{-1} after heating and cooling treatment (Table S3). The ϕ values were determined to be 4.0×10^{-3} % before and after heating and cooling treatment by current integration of TOF transients after heating. Accordingly, the hole mobilities of ZnPc-ref were obtained as 7.3 cm^2 V^{-1} s^{-1} before heating and 3.0 cm^2 V^{-1} s^{-1} after heating and cooling treatment (Table 1). The larger value before heating than after heating and cooling treatment may result from the crystallinity nature of ZnPc-ref. That is, the annealing process of ZnPc-ref molecules causes transformation of crystal to liquid crystal, yielding the drops in the TRMC transient and the hole mobility. On the other hand, ZnPc−C_{60} exhibits maximum transient conductivities of 5.3×10^{-5} cm^2 V^{-1} s^{-1} before heating and of 1.5×10^{-4} cm^2 V^{-1} s^{-1} after heating and cooling treatment. From the ϕ values (5.2×10^{-2} % before heating, 2.9×10^{-2} % after heating and cooling treatment) of ZnPc−C_{60} (Table S3), the charge mobilities of ZnPc−C_{60} were obtained as 0.10 cm^2 V^{-1} s^{-1} before heating and of 0.52 cm^2 V^{-1} s^{-1} after heating and cooling treatment (Table 1). These short-range trends are consistent with long-range trends observed by the TOF method. These prompt increases of transient conductivities for the ZnPc-ref and ZnPc−C_{60} films arise from the photoresponse behavior of these films, in which free charge carriers, defined as charges escaped from the recombination process, are generated by laser excitation. In the decay part of the transient conductivity, the carriers are distributed randomly in the film and subsequently undergo recombination.[16]

It should be noted that TRMC signals consist of the sum of charge mobilities for the negative and positive carriers, and we cannot extract respective electron and hole mobilities from the TRMC value accurately. The ZnPc-ref has a much higher TRMC charge mobility than does the ZnPc−C_{60} molecule. The presence of C_{60} moiety in the ZnPc−C_{60} film may disorder the ZnPc arrangement in the ZnPc−C_{60} column, lowering the TRMC value, especially the hole mobility.[12] In the TOF measurements, the ZnPc−C_{60} film exhibits high hole (0.26 cm^2 V^{-1} s^{-1}) and electron (0.11 cm^2 V^{-1} s^{-1}) mobilities, the hole mobility being ~2 times larger than the electron mobility. Thus, both charge mobilities would contribute to the TRMC value of ZnPc−C_{60} because of the comparable electron and hole mobilities of ZnPc−C_{60} obtained by the TOF measurements as well as the expected short-range TRMC charge mobilities ($\geq$0.11 cm^2 V^{-1} s^{-1}), which are typically higher than the long-range TOF charge mobilities. Some previous papers suggested that co-assembly of a D−A linked dyad with corresponding D or A molecules allows better packing of the molecular units and results in larger charge mobilities.[9b,17] We may be able to improve the charge-transport properties of ZnPc−C_{60} by blending suitable phthalocyanine or fullerene derivatives.

Considering that TRMC and TOF measurements provide short-range and long-range charge-transport properties, respectively, TRMC values depend on the degree of alignment for ZnPc−C_{60} molecules in the ZnPc−C_{60} intracolumn, whereas TOF values correlate with that between ZnPc−C_{60} intercolumns as well as in the ZnPc−C_{60} intracolumn. Note that the μ_h and μ_e values measured by TOF after heating are 26 and 7 times higher than those before heating, respectively. On the other hand, the total charge mobility measured by TRMC after the heating and cooling treatment is 5 times higher than that before heating. It is evident that the enhancement in the total charge mobility obtained by TOF is larger than that obtained by TRMC. More well-ordered alignment of the respective ZnPc−C_{60} columns in the LC after heating may facilitate intracharge transport between the ZnPc−C_{60} columns, leading to the improvement of the macroscopic charge mobilities.

In conclusion, we have successfully prepared a promising type of D−A linked dyad that is self-assembled to form segregated D−A columns in liquid crystals. The D−A heterojunction structure of ZnPc−C_{60} molecules was found to exhibit highly efficient ambipolar charge-transport properties. This relationship between the LC structures and charge-transport properties will provide basic and fundamental information on the rational design of high-performance LC materials for use in organic electronics.

■ ASSOCIATED CONTENT

Supporting Information. Complete ref 5a, experimental details, schemes, tables, and additional figures. This material is available free of charge via the Internet at http://pubs.acs.org.

AUTHOR INFORMATION

Corresponding Author
seki@chem.eng.osaka-u.ac.jp; yo-shimizu@aist.go.jp; imahori@scl.kyoto-u.ac.jp

ACKNOWLEDGMENT

This work was supported by Grant-in-Aid (No. 21350100 to H.I.) and WPI Initiative, MEXT, Japan. H.H. is grateful for a JSPS fellowship for young scientists.

REFERENCES

(1) (a) Shimizu, Y.; Oikawa, K.; Nakayama, K.; Guillon, D. *J. Mater. Chem.* **2007**, *17*, 4223. (b) Rosen, B. M.; Wilson, C. J.; Wilson, D. A.; Peterca, M.; Imam, M. R.; Percec, V. *Chem. Rev.* **2009**, *109*, 6275.

(2) (a) Laschat, S.; Baro, A.; Steinke, N.; Giesselmann, F.; Hägele, C.; Scalia, G.; Judele, R.; Kapatsina, E.; Sauer, S.; Schreivogel, A.; Tosoni, M. *Angew. Chem., Int. Ed.* **2007**, *46*, 4832. (b) Kato, T.; Yasuda, T.; Kamikawa, Y.; Yoshio, M. *Chem. Commun.* **2009**, 729.

(3) (a) Percec, V.; Gloddle, M.; Bera, T. K.; Miura, Y.; Shiyanovskaya, I.; Singer, K. D.; Balagurusamy, V. S. K.; Heiney, P. A.; Schnell, I.; Rapp, A.; Spiess, H. -W.; Hudson, S. D.; Duan, H. *Nature* **2002**, *419*, 384. (b) Samori, P.; Yin, X.; Tchebotareva, N.; Wang, Z.; Pakula, T.; Jäckel, F.; Watson, M. D.; Venturini, A.; Müllen, K.; Rabe, J. P. *J. Am. Chem. Soc.* **2004**, *126*, 3567. (c) Pisula, W.; Kastler, M.; Wasserfallen, D.; Robertson, J. W. F.; Nolde, F.; Kohl, C.; Müllen, K. *Angew. Chem., Int. Ed.* **2006**, *45*, 819. (d) Tasios, N.; Grigoriadis, C.; Hansen, M. R.; Wonneberger, H.; Li, C.; Spiess, H. W.; Müllen, K.; Floudas, G. *J. Am. Chem. Soc.* **2010**, *132*, 7478.

(4) (a) Shi, Q.; Hou, Y.; Jin, H.; Li, Y. *J. Appl. Phys.* **2007**, *102*, 073108. (b) Ballantyne, A. M.; Chen, L.; Dane, J.; Hammant, T.; Braun, F. M.; Heeney, M.; Duffy, W.; McCulloch, I.; Bradley, D. D. C.; Nelson, J. *Adv. Funct. Mater.* **2008**, *18*, 2373. (c) Li, W. -S.; Yamamoto, Y.; Fukushima, T.; Saeki, A.; Seki, S.; Tagawa, S.; Masunaga, H.; Sasaki, S.; Takata, M.; Aida, T. *J. Am. Chem. Soc.* **2008**, *130*, 8886. (d) Bullock, J. E.; Carmieli, R.; Mickley, S. M.; Vura-Weis, J.; Wasielewski, M. R. *J. Am. Chem. Soc.* **2009**, *131*, 11919. (e) Charvet, R.; Acharya, S.; Hill, J. P.; Akada, M.; Liao, M.; Seki, S.; Honsho, Y.; Saeki, A.; Ariga, K. *J. Am. Chem. Soc.* **2009**, *131*, 18030. (f) Hizume, Y.; Tashiro, K.; Charvet, R.; Yamamoto, Y.; Saeki, A.; Seki, S.; Aida, T. *J. Am. Chem. Soc.* **2010**, *132*, 6628.

(5) (a) Imahori, H.; et al. *Chem.—Eur. J.* **2007**, *13*, 10182. (b) Kira, A.; Umeyama, T.; Matano, Y.; Yoshida, K.; Isoda, S.; Park, J. K.; Kim, D.; Imahori, H. *J. Am. Chem. Soc.* **2009**, *131*, 3198. (c) Umeyama, T.; Tezuka, N.; Kawashima, F.; Seki, S.; Matano, Y.; Nakao, Y.; Shishido, T.; Nishi, M.; Hirao, K.; Lehtivuori, H.; Tkachencko, N. V.; Lemmetyinen, H.; Imahori, H. *Angew. Chem., Int. Ed.* **2011**, *50*, 4615.

(6) Hanack, M.; Lang, M. *Adv. Mater.* **1994**, *6*, 819.

(7) (a) Nierengarten, J. -F.; Solladie, N.; Deschenaux, R. In *Fullerenes*; Langa, F., Nierengarten, J.-F., Eds.; RSC Publishing: Cambridge, 2007; Chapter 5. (b) Campidelli, S.; Bourgun, P.; Guintchin, B.; Furrer, J.; Stoeckli-Evans, H.; Saez, I. M.; Goodby, J. W.; Deschenaux, R. *J. Am. Chem. Soc.* **2010**, *132*, 3574.

(8) (a) Lenoble, J.; Campidelli, S.; Maringa, N.; Donnio, B.; Guillon, D.; Yevlampieva, N.; Deschenaux, R. *J. Am. Chem. Soc.* **2007**, *129*, 9941. (b) Lenoble, J.; Maringa, N.; Campidelli, S.; Donnio, B.; Guillon, D.; Deschenaux, R. *Org. Lett.* **2006**, *8*, 1851. (c) Maringa, N.; Lenoble, J.; Donnio, B.; Guillon, D.; Deschenaux, R. *J. Mater. Chem.* **2008**, *18*, 1524. (d) Hoang, T. N. Y.; Pociecha, D.; Salamonczyk, M.; Gorecka, E.; Deschenaux, R. *Soft Matter* **2011**, *7*, 4948.

(9) (a) Bottari, G.; de la Torres, G.; Guldi, D. M.; Torres, T. *Chem. Rev.* **2010**, *110*, 6768. (b) de la Escosura, A.; Matínez-Díaz, M. V.; Barberá, J.; Torres, T. *J. Org. Chem.* **2008**, *73*, 1475. (c) Geerts, Y. H.; Debever, O.; Amato, C.; Sergeyev, S. *Beilstein J. Org. Chem.* **2009**, *5*, DOI: 10.3762/bjoc.5.49. (d) Ince, M.; Martínez-Díaz, M. V.; Barberá, J.; Torres, T. *J. Mater. Chem.* **2011**, *21*, 1531.

(10) Ichihara, M.; Suzuki, A.; Hatsusaka, K.; Ohta, K. *Liq. Cryst.* **2007**, *34*, 555.

(11) (a) Iino, H.; Takayashiki, J.; Hanna, J.; Bushby, R. J. *Jpn. J. Appl. Phys.* **2005**, *44*, L1310. (b) Iino, H.; Hanna, J.; Bushby, R. J.; Movaghar, B.; Whitaker, B. J.; Cook, M. J. *Appl. Phys. Lett.* **2005**, *7*, 132102. (c) Miyake, Y.; Shiraiwa, Y.; Okada, K.; Monobe, H.; Hori, T.; Yamasaki, N.; Yoshida, H.; Cook, M. J.; Fujii, A.; Ozaki, M.; Shimizu, Y. *Appl. Phys. Express* **2011**, *4*, 021604.

(12) On the basis of the Col_r2 structure for ZnPc−C_{60}, the ZnPc plane is tilted by 7.4° against the axis of the ZnPc column. Given that the C_{60} helical pitch is 16 times the layer spacing, the separation distance between the C_{60} (0.7−0.9 nm) is estimated to be smaller than the shortest one between the C_{60} (∼1.0 nm). Such enhanced packing of the C_{60} may be achieved by the disordered wedge-shaped open stacked ZnPc in the ZnPc column.

(13) (a) Barberá, J.; Cavero, E.; Lehmann, M.; Serrano, J.; Sierra, T.; Vázquez, J. T. *J. Am. Chem. Soc.* **2003**, *125*, 4527. (b) Pisula, W.; Tomovic, Z.; Simpson, C.; Kastler, M.; Pakula, T.; Müllen, K. *Chem. Mater.* **2005**, *17*, 4296. (c) Lee, S.; Lin, H.; Lin, Y.; Chen, H.; Liao, C.; Lin, T.; Chu, Y.; Hsu, H.; Chen, C.; Lee, J.; Hung, W.; Liu, Q.; Wu, C. *Chem.—Eur. J.* **2011**, *17*, 792.

(14) (a) Seki, S.; Yoshida, Y.; Tagawa, S.; Asai, K.; Ishigure, K.; Furukawa, K.; Fujiki, M.; Matsumoto, N. *Philos. Mag. B* **1999**, *79*, 1631. (b) Kunimi, Y.; Seki, S.; Tagawa, S. *Solid State Commun.* **2000**, *114*, 469.

(15) Saeki, A.; Seki, S.; Koizumi, Y.; Sunagawa, T.; Ushida, K.; Tagawa, S. *J. Phys. Chem. B* **2005**, *109*, 10015.

(16) (a) Saeki, A.; Seki, S.; Sunagawa, T.; Ushida, K.; Tagawa, S. *Philos. Mag.* **2006**, *86*, 1261. (b) Saeki, A.; Seki, S.; Tagawa, S. *J. Appl. Phys.* **2006**, *100*, 023703.

(17) (a) Goldmann, D.; Janietz, D.; Schmidt, C.; Wendorff, J. H. *Angew. Chem., Int. Ed.* **2000**, *39*, 1851. (b) Reczek, J. J.; Villazor, K. R.; Lynch, V.; Swager, T. M.; Iverson, B. L. *J. Am. Chem. Soc.* **2006**, *128*, 7995.